Luminescent Amphiphilic Aminoglycoside Probes to Study Transfection

Alexander Zimmermann[+],[a] Qais Z. Jaber[+],[d] Johannes Koch,[b] Steffen Riebe,[a] Cecilia Vallet,[c] Kateryna Loza,[e] Matthias Hayduk,[a] Kfir B. Steinbuch,[d] Shirley K. Knauer,[c] Micha Fridman,*[d] and Jens Voskuhl*[a]

In memory of Prof. Dr. Carsten Schmuck (1968–2019).

We report the characterization of amphiphilic aminoglycoside conjugates containing luminophores with aggregation-induced emission properties as transfection reagents. These inherently luminescent transfection vectors are capable of binding plasmid DNA through electrostatic interactions; this binding results in an emission "on" signal due to restriction of intramolecular motion of the luminophore core. The luminescent cationic amphiphiles effectively transferred plasmid DNA into mammalian cells (HeLa, HEK 293T), as proven by expression of a red fluorescent protein marker. The morphologies of the aggregates were investigated by microscopy as well as ζ-potential and dynamic light-scattering measurements. The transfection efficiencies using luminescent cationic amphiphiles were similar to that of the gold-standard transfection reagent Lipofectamine® 2000.

[a] *A. Zimmermann,[+] S. Riebe, M. Hayduk, Jun.-Prof. J. Voskuhl*
Faculty of chemistry (Organic Chemistry) and
Centre for Nanointegration Duisburg-Essen (CENIDE)
University of Duisburg-Essen
Universitätsstrasse 7, 45117 Essen (Germany)
E-mail: jens.voskuhl@uni-due.de
[b] *Dr. J. Koch*
Center for Medical Biotechnology (ZMB), University of Duisburg Essen
Universitätsstrasse 2, 45141 Essen (Germany)
[c] *Dr. C. Vallet, Prof. S. K. Knauer*
Institute for Molecular Biology
Centre for Medical Biotechnology (ZMB), University of Duisburg-Essen
Universitätsstrasse 2, 45117 Essen (Germany)
[d] *Q. Z. Jaber,[+] Dr. K. B. Steinbuch, Prof. M. Fridman*
School of Chemistry
Raymond and Beverly Sackler Faculty of Exact Sciences
Tel Aviv University
Tel Aviv 6997801 (Israel)
E-mail: mfridman@tauex.tau.ac.il
[e] *Dr. K. Loza*
Inorganic Chemistry and Centre for Nanointegration Duisburg-Essen (CeNIDE)
University of Duisburg-Essen
Universitätsstrasse 7, 45141 Essen (Germany)
[+] *These authors authors contributed equally to this work.*

Supporting information for this article is available on the WWW under https://doi.org/10.1002/cbic.202000725

Genetic engineering has been one of the foundations of biological and medical research for decades. For example, plants and animals can be genetically engineered to render them immune to various diseases or extreme climate conditions.[1] In addition, various hereditary diseases caused by DNA damage can be treated with gene therapy, emphasizing the tremendous potential and utilities of these approaches for the benefit of humankind.[2]

In 2013 the CRISPR-Cas9[3] method was first introduced and has rapidly become a powerful tool for DNA editing. This method makes it possible to remove specific DNA sequences or insert exogenous genetic material into the existing genetic code. The CRISPR-Cas9-based system has enormous potential to treat diseases that are caused by DNA damage[4] or to modify genetic codes[5] but its components must be transported into cells by transfection.[6]

Approaches for transfer genetic material into cells include physical,[7] biological[8] and chemical methods.[9] Transfection *via* nanoparticles,[10] cationic polymers,[11] calcium phosphate precipitation[12] and lipofection[13] are among the chemical processes. Unfortunately though, efficient transfection is often accompanied with high toxicity.[14]

Small-molecule-based amphiphiles have also been used to induce the transport of genetic material into cells by the so called "lipofection" process.[13] Self-assemblies bearing cationic charges[15] that capture DNA fragments are efficiently taken up into cells through an endocytotic pathway followed by lysosomal escape.[16] Steroid-based hydrophobic anchors, such as cholesterol, have proven to be important components of amphiphilic transfection reagents as steroids are essential constituents of mammalian membranes.[17] Small-molecule-based transfection reagents with linear,[18] branched,[19] peptide-based (oligo)amines,[20] imidazolium units[21] or oxo-anion binders[22] hydrophilic groups have been described. Aminoglycosides are an important class of pseudo-oligosaccharide antibiotics that are highly positively charged under physiological conditions.[23] Lehn and co-workers[24] showed that aminoglycosides linked to cholesterol are efficient transfection vectors. Huang and co-workers[25] and Lehn and co-workers[26] reported that variations of the hydrophobic moiety had an immense influence on the transfection ability of cationic amphiphiles.

To facilitate the ability to track transfection agents inside a cell and characterize the transfection process we were interested in developing inherently luminescent transfection agents and use them for studying the transfection process in live mammalian cells.

In this study we designed and synthesized amphiphilic transfection agents composed of the aminoglycoside tobramycin, which has a net positive charge of +5 under physiological conditions and hydrophobic aggregation-induced emission (AIE) cores to form AIE luminophore-based transfection reagents. Very recently we were able to show that an estrone-based AIE luminophore coupled with an oligoamine is capable of emission enhancement upon plasmid DNA binding due to crosslinking of self-assembled structures and has modest transfection properties.[27] Unlike classic luminophores, which lose their emission upon aggregation due to nonradiative pathways, the AIE effect is observed for phenyl-rotor containing compounds that induce emission when the luminophore is entrapped in a sterically constrained environment.[28]

Compounds **1** and **2** (Figure 1) were synthesized by coupling of the AIE-active cores bearing either estrone[27] or a simple phenyl-moiety as hydrophobic anchor cores to the protected aminoglycoside[29] followed TFA removal of the BOC-protection groups and HPLC purification (for detailed synthetic procedure and structural characterization see the Supporting Information).

Both amphiphiles **1** and **2** were found to be readily soluble in water and displayed only negligible emission (λ_{em} = 480–500 nm) over a large concentration range (Figure S5). To search for self-assemblies or aggregates in aqueous media at higher concentrations we conducted a Nile Red (NR) assay to determine the critical aggregation concentration (CAC). NR is not emissive in aqueous media due to self-quenching upon aggregation.[30] When entrapped in a hydrophobic environment an emission increase is observed at around 650 nm, which makes it the ideal reporter dye for tracking assembly processes. The CAC of compound **1** could not have been determined whereas for compound **2** a CAC was determined to be 9 ± 1 μM, which emphasizes the more hydrophobic character of this compound (*vide infra*; Figure S7).

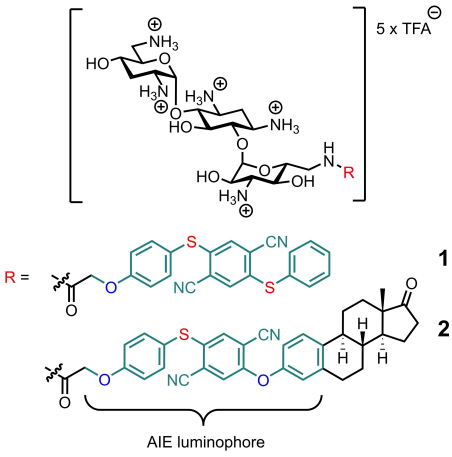

Figure 1. Molecular structure of luminescent amphiphilic tobramycins **1** and **2**. The AIE-active part of the molecule is shown in turquoise.

To evaluate the binding efficacy of plasmid DNA to amphiphiles **1** and **2** we investigated how the optical density at 500 nm changes upon addition of pH2B-mRFP plasmid to a solution containing the amphiphiles. Multiple electrostatic interactions between the cationic aminoglycoside head-group of **1** and **2** and the phosphate backbone of the plasmid DNA should lead to formation of noncovalent ionic-interactions-based lipoplexes which should result in increased turbidity (Figure 2A). For both **1** and **2** a significant increase in optical density was observed which confirmed the formation of lipoplexes. The higher turbidity for compound **2** can be attributed to the increased hydrophobicity of this compound. To support this hypothesis, the distribution coefficient (log *D*) a lipophilicity descriptor, taking the partition of the ionized and non-ionized forms of the two cationic amphiphiles was calculated. As indicated by the calculated log *D* values, compound **2** is about two orders of magnitude more hydrophobic than **1** (log *D* values of −6.36 and −8.31, respectively). Binding to plasmid DNA, as detected by reaching a plateau in optical density, was slower for **2** and reached equilibrium after 20 minutes. This behavior may be attributed to densely packed structures of the more hydrophobic cationic amphiphile **2**.

Attempts to visualize the morphologies formed by **2** using advanced microscopy techniques such as STEM or AFM failed. It is assumed that the self-assembled structures of **2** were not stable enough to be visualized, likely due to the sample preparation conditions, such as spin-coating (Figure 2B and the Supporting Information).

The assemblies, consisting of amphiphiles **1** or **2** and plasmid DNA, were also investigated by AFM and STEM measurements, revealing large aggregates of several micrometers (Figure 2B). It is noteworthy that the structures observed consist of clustered smaller aggregates, which was attributed to the sample preparation, since dried samples obtained by drop casting or spin-coating force the assemblies to aggregate (Figure 2B). Additionally the plasmid DNA was also measured by using STEM and AFM revealing small particles or rod-like structures as expected for plasmid DNA (Figure S16). Hence we assume that the aggregates formed by **1** and **2** consist of condensed DNA, able to be transported into cells. To determine the size in solution, additional DLS measurements were conducted, revealing a size increase of the preformed assemblies of **1** and **2** to more than 100 nm (size distribution by volume) upon plasmid addition, supporting the hypothesis, that the assemblies observed in STEM and AFM consist of smaller clustered structures (Figures S14 and S15).

We next investigated the assembly behavior of **1** and **2** in an aqueous solution and evaluated their photophysical properties in the presence and absence of plasmid DNA (pH2B-mRFP). Hence, we carried out a concentration-dependent study of emission properties (Figure 2C and D). We assumed that due to the amphiphilic nature of **1** and **2** they are likely to self-assemble at higher concentrations and that this should lead to an increase in emission due to a restriction of motion.

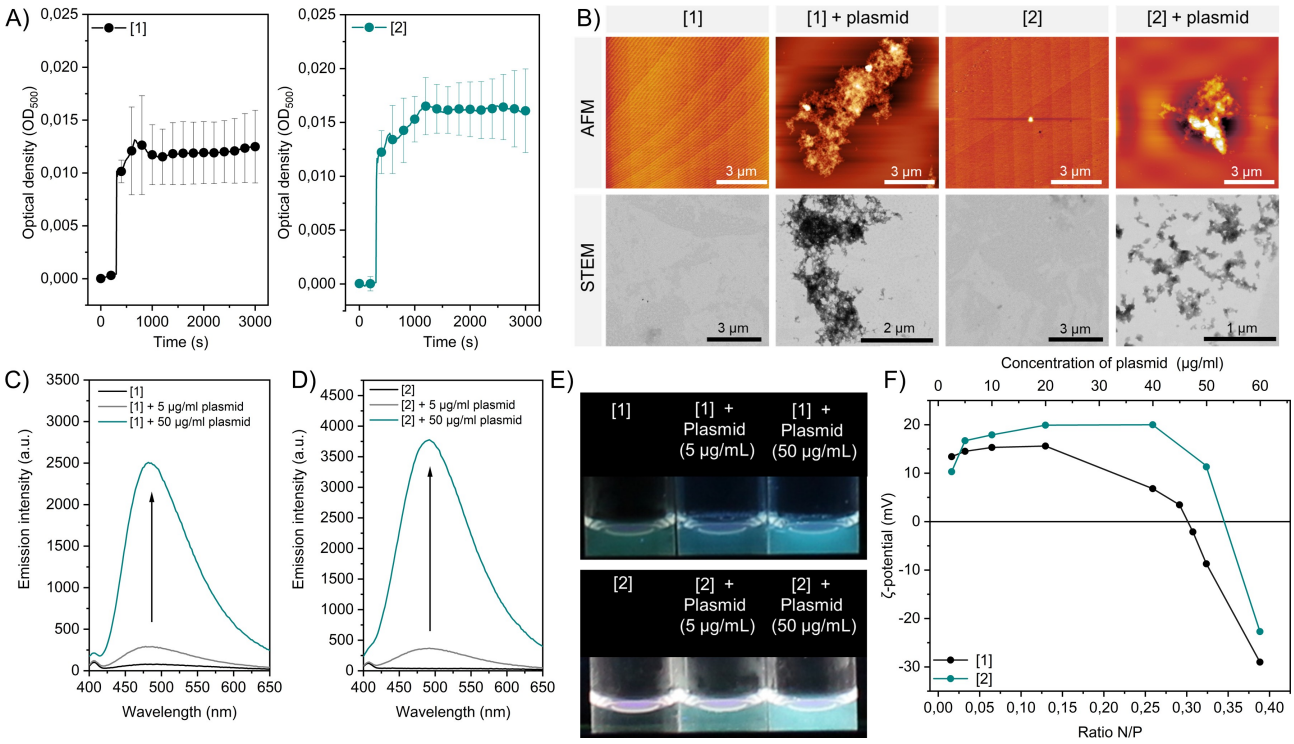

Figure 2. A) Increase in optical density upon the addition of plasmid DNA at 500 nm as determined by UV/Vis spectroscopy, concentration **1** = **2** = 100 µM, concentration (plasmid) = 10 µg/mL, measured in triplicate. B) AFM and STEM images of **1** and **2** in the presence of plasmid DNA, concentrations as in (A). Emission enhancement upon the addition of different concentrations of plasmid DNA to C) **1** or D) **2** (50 µM), E) Photographs of **1** and **2** in the presence and absence of plasmid DNA, concentration of **1** = **2** = 50 µM under UV-light excitation (λ_{ex} = 365 nm). F) ζ-Potential changes upon the addition of plasmid DNA to a fixed concentration (100 µM) of **1** and **2** versus the ratio of negative and positive (N/P) charges in the system and the concentration of plasmid DNA (for calculation details please see the Supporting Information), Samples of compound **1** and **2** were prepared from DMSO stock solutions (40 mM).

Pronounced emission enhancement of up to the factor of ten was observed upon addition of plasmid DNA to amphiphiles **1** and **2** (Figure 2C and D). This enhancement in emission supports the assumption, that electrostatic non-covalent cross-linking leads to a higher restriction of motion inducing emission by the AIE-active cores of the two amphiphiles. This effect was significant enough to be detected by bare eye (Figure 2E) under UV-light excitation (λ_{ex} = 365 nm, λ_{em} = 470–490 nm) which was more pronounced for **2** (50% higher emission intensity compared to **1**; Figure 2C and D). This observation can be attributed to the higher hydrophobicity of **2**, enabling a denser packing and hence an improved restriction of motion. This suggested to us that AIE-based cationic amphiphiles **1** and **2** should be useful for visualization of transfection processes in cells. Furthermore, a concentration dependent investigation of the ζ-potential of the lipoplexes (constant concentration of compound **1** and **2** while varying plasmid concentration) revealed, that these amphiphiles invert their surface potential due to charge neutralization at higher plasmid concentrations. Assuming two negative charges per base pair in the DNA and five positive charges per monomer of **1** and **2**, we calculated a ζ-potential of zero at a ratio of negative to positive charges (N/P) of around 0.3 (Figure 2F). This led to the assumption that an excess of positive charges is needed to neutralize the aggregates formed by **1** and **2** (Figure 2F) and plasmid DNA. To visually investigate and characterize the transfection properties of **1** and **2**, lipoplexes composed of these amphiphiles and plasmid DNA, coding for the nuclear histone protein H2B linked to a C-terminal red fluorescent protein (pH2B-mRFP), were introduced to two different cell lines (HeLa and HEK 293T, Figure 3). Firstly, the cytotoxicity of both compounds was investigated using a MTS cell proliferation assay and was found to be low with cell viability exceeding 80% even at 100 µM of the amphiphiles (Figure 4A). To ensure minimal toxicity we focused on a concentration range below 100 µM. Transfection efficacy was evaluated by quantifying the expression of the red

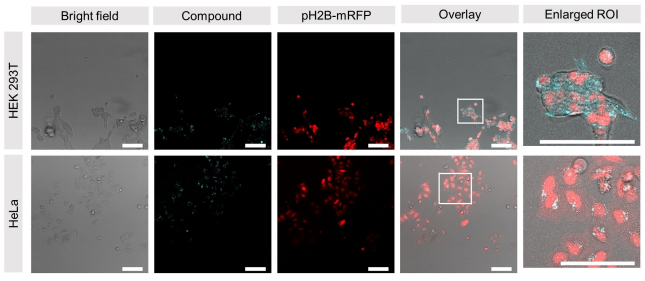

Figure 3. Microscopy images (CLSM) of HEK 293T and HeLa cells 16 h after transfection with **2** (47.6 µM, turqoise) premixed with pH2B-mRFP plasmid (2.4 µg/mL, red). Scale bars: 100 µm, for details see the Supporting Information. Compound **2** was added from a stock solution in DMSO (40 mM).

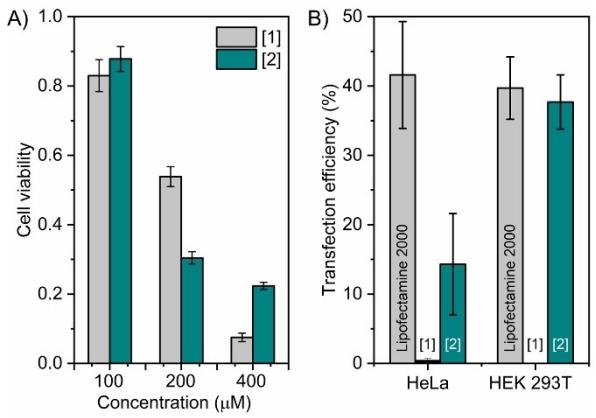

Figure 4. A) Cell viability (MTS cell proliferation assay) of HeLa cells with different concentrations of **1** and **2**. B) Transfection efficiency of **1** and **2** for HeLa and HEK 293T cells. Concentration **1** = **2** = 47.6 μM, [pH2B-mRFP plasmid] = 2.4 μg/mL. Lipofectamine® 2000 is shown for comparison. Volume (Lipofectamine® 2000) = 1 μL, [pH2B-mRFP plasmid] = 500 ng/50 μL medium. Compounds **1** and **2** were added from stock solutions in DMSO (40 mM).

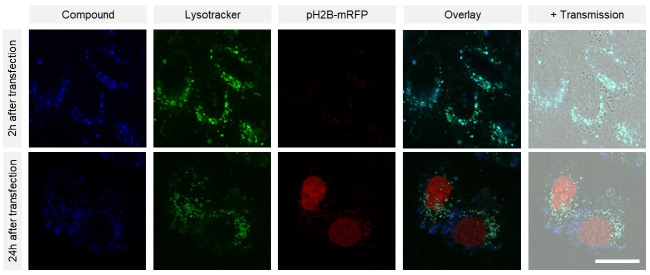

Figure 5. Microscopy images (CLSM) of HeLa cells 2 and 24 h after transfection with **2** (47.6 μM, dark blue) premixed with pH2B-mRFP plasmid (2.4 μg/mL, red) and stained with LysoTracker™ Green. Scale bar: 20 μm, for details see the Supporting Information. Compound **2** was added from a stock solution in DMSO (40 mM).

fluorescent protein inside the nucleus monitored by confocal laser scanning microscopy and compared with the gold standard transfection agent Lipofectamine® 2000. Subcellular distribution of **1** and **2** was determined by fluorescent microscopy (λ_{ex} = 405 nm; λ_{em} = 470–490 nm, Figures 3, S9, and S10).

Lipoplexes of **1** and **2** were efficiently taken up by mammalian cells (HeLa, HEK 293T; blue fluorescence inside the cells, Figure 3, overlay image, Figures S9 and S10).

To our surprise only compound **2** was able to successfully transfect the plasmid DNA as evident by the red fluorescent emission in the nuclei as a result of the expression of pH2B-mRFP (Figures 3 and S9). Only marginal transfection rates were observed for compound **1** (Figure S10).

As a positive control, transfection was carried out using the commercial agent Lipofectamine® 2000 (Figure S9) in HeLa and HEK 293T cells.

The comparison of **2** with Lipofectamine 2000® revealed similar transfection efficiencies in HEK 293T cells, with a transfection efficiency of nearly 38% for compound **2** and 40% for Lipofectamine® 2000.

Transfection efficacy was determined by co-staining of the cells with SYTO 61 nuclear stain (λ_{ex} = 633 nm) as commonly used dyes like Hoechst overlap with the emission of the compounds. The ratio between the number of pH2B-mRFP expressing and all cells (segmented by the SYTO 61 intensity) was calculated (For details see the Supporting Information and Figure S13). Notably, transfection efficacy of **2** in HeLa cells was 34% of that induced by Lipofectamine® 2000 (14% (**2**) and 41% (Lipofectamine® 2000)), respectively (Figure 4B).

To investigate the potential mode of uptake, distribution and transfection, we carried out subcellular localization microscopy experiments using LysoTracker™ Green in the presence of lipoplexes composed of **1** or **2** and plasmid DNA (Figures 5, S11 and S12). Compounds **1** and **2** localized largely to lysosomes 2 h after their introduction to the cells, suggesting that the lipoplexes of these amphiphiles enter cells *via* the endosomal pathway.

Interestingly, after 24 h, the blueish signal of the lipoplexes faded and labeled the cytosol, indicating a lysosomal escape process followed by successful transfection (Figures 5, S11 and S12).

The fact that the estrone core motif of **2** ($\log D = -6.36$) is more hydrophobic than that of **1** ($\log D = -8.31$) suggests that membrane integration of lipoplexes of **2** followed by their endocytosis and lysosomal release is favorable compared to those achieved by lipoplexes of **1** and may explain the superior transfection properties of **2**.

To conclude, we have designed and synthesized a unique type of transfection agents composed of luminophores with aggregation-induced emission (AIE) properties and the aminoglycoside tobramycin. The emission "on" state of these unique cationic amphiphiles upon plasmid binding was used to track the transfection process in mammalian cells and revealed an endocytotic uptake process accompanied by lysosomal escape into the cytosol. By combining fluorescent tracking and efficient transfection amphiphilic-aminoglycoside-based transfection agents offer useful tools for the study cellular uptake of genetic material.

Acknowledgments

The authors acknowledge the Center for Nanointegration (CENIDE), the Imaging Centre Campus Essen (ICCE) and the Center of Medical Biotechnology (ZMB). This work was also supported by the Israel Science Foundation, grant no. 179/19 (to M.F.). Q.Z.J. thanks the Israel Council for Higher Education for the scholarship granted to outstanding doctoral students. We thank furthermore Kevin Rudolph for help with the AFM measurements. Open access funding enabled and organized by Projekt DEAL.

Conflict of Interest

The authors declare no conflict of interest.

Keywords: aggregation-induced emission · bioimaging · cationic amphiphiles · self-assembly · transfection agents

[1] a) Z. K. Punja, *Can. J. Plant Pathol.* **2001**, *23*, 216–235; b) P. Jeandet, C. Clement, E. Courot, S. Cordelier, *Int. J. Mol. Sci.* **2013**, *14*, 14136–14170; c) C. B. Whitelaw, H. M. Sang, *Rev. Sci. Tech.* **2005**, *24*, 275–283.
[2] a) D. L. Knoell, I. M. Yiu, *Am. J. Health-Syst. Pharm.* **1998**, *55*, 899–904; b) M. D. Hoban, S. H. Orkin, D. E. Bauer, *Blood* **2016**, *127*, 839–848; c) X. M. Anguela, K. A. High, *Annu. Rev. Med.* **2019**, *70*, 273–288.
[3] a) E. Charpentier, J. A. Doudna, *Nature* **2013**, *495*, 50–51; b) L. Cong, F. A. Ran, D. Cox, S. L. Lin, R. Barretto, N. Habib, P. D. Hsu, X. B. Wu, W. Y. Jiang, L. A. Marraffini, F. Zhang, *Science* **2013**, *339*, 819–823.
[4] a) X. Dagenais-Lussier, H. Loucif, A. Murira, X. Laulhé, S. Stäger, A. Lamarre, J. Van Grevenynghe, *Viruses* **2018**, *10*, 12; b) M. Yanik, B. Müller, F. Song, J. Gall, F. Wagner, W. Wende, B. Lorenz, K. Stieger, *Prog. Retinal Eye Res.* **2017**, *56*, 1–18.
[5] a) J. E. DiCarlo, J. E. Norville, P. Mali, X. Rios, J. Aach, G. M. Church, *Nucleic Acids Res.* **2013**, *41*, 4336–4343; b) H. Yang, H. Wang, R. Jaenisch, *Nat. Protoc.* **2014**, *9*, 1956–1968; c) H. Puchta, *Curr. Opin. Plant Biol.* **2017**, *36*, 1–8.
[6] C. A. Lino, J. C. Harper, J. P. Carney, J. A. Timlin, *Drug Delivery* **2018**, *25*, 1234–1257.
[7] H. Potter, R. Heller, *Curr. Protoc. Mol. Biol.* **2018**, *121*, 9 3 1–9 3 13.
[8] E. Wagner, M. Zenke, M. Cotten, H. Beug, M. L. Birnstiel, *Proc. Nati. Acad. Sci. USA* **1990**, *87*, 3410–3414.
[9] A. K. Fajrial, Q. Q. He, N. I. Wirusanti, J. E. Slansky, X. Ding, *Theranostics* **2020**, *10*, 5532–5549.
[10] a) K. K. Sandhu, C. M. McIntosh, J. M. Simard, S. W. Smith, V. M. Rotello, *Bioconjugate Chem.* **2002**, *13*, 3–6; b) S. Prabha, W.-Z. Zhou, J. Panyam, V. Labhasetwar, *Int. J. Pharm.* **2002**, *244*, 105–115.
[11] a) S. C. De Smedt, J. Demeester, W. E. Hennink, *Pharm. Res.* **2000**, *17*, 113–126; b) B. R. Olden, Y. Cheng, J. L. Yu, S. H. Pun, *J. Controlled Release* **2018**, *282*, 140–147.
[12] R. E. Kingston, C. A. Chen, J. K. Rose, *Curr. Protoc. Mol. Biol.* **2003**, *Chapter 9*, Unit 9 1.
[13] P. L. Felgner, T. R. Gadek, M. Holm, R. Roman, H. W. Chan, M. Wenz, J. P. Northrop, G. M. Ringold, M. Danielsen, *Proc. Nati. Acad. Sci. USA* **1987**, *84*, 7413–7417.
[14] A. Masotti, G. Mossa, C. Cametti, G. Ortaggi, A. Bianco, N. D. Grosso, D. Malizia, C. Esposito, *Colloids Surf. B. Biointerfaces* **2009**, *68*, 136–144.
[15] D. Fischer, T. Bieber, Y. Li, H.-P. Elsässer, T. Kissel, *Pharm. Res.* **1999**, *16*, 1273–1279.
[16] M. Savva, P. Chen, A. Aljaberi, B. Selvi, M. Spelios, *Bioconjugate Chem.* **2005**, *16*, 1411–1422.
[17] M. D. Kearns, A.-M. Donkor, M. Savva, *Mol. Pharm.* **2008**, *5*, 128–139.
[18] B. Brissault, A. Kichler, C. Guis, C. Leborgne, O. Danos, H. Cheradame, *Bioconjugate Chem.* **2003**, *14*, 581–587.
[19] Y.-X. Sun, B. Yang, S. Chen, Q. Lei, J. Feng, X.-F. Qiu, N.-G. Dong, R.-X. Zhuo, X.-Z. Zhang, *Colloids Surf. B. Biointerfaces* **2013**, *111*, 732–740.
[20] Y.-W. Won, H. A. Kim, M. Lee, Y.-H. Kim, *Mol. Ther.* **2010**, *18*, 734–742.
[21] T. O. Paulisch, S. Bornemann, M. Herzog, S. Kudruk, L. Roling, A. L. Linard Matos, H.-J. Galla, V. Gerke, R. Winter, F. Glorius, *Chem. Eur. J.* **2020**, *26*, 17176–17182.
[22] A. Gigante, M. Li, S. Junghänel, C. Hirschhäuser, S. Knauer, C. Schmuck, *MedChemComm* **2019**, *10*, 1692–1718.
[23] a) Q. Z. Jaber, R. I. Benhamou, I. M. Herzog, B. Ben Baruch, M. Fridman, *Angew. Chem. Int. Ed.* **2018**, *57*, 16391–16395; b) J. C. K. Quirke, P. Rajasekaran, V. A. Sarpe, A. Sonousi, I. Osinnii, M. Gysin, K. Haldimann, Q.-J. Fang, D. Shcherbakov, S. N. Hobbie, S.-H. Sha, J. Schacht, A. Vasella, E. C. Böttger, D. Crich, *J. Am. Chem. Soc.* **2020**, *142*, 530–544; c) S. L. Zada, B. B. Baruch, L. Simhaev, H. Engel, M. Fridman, *J. Am. Chem. Soc.* **2020**, *142*, 3077–3087.
[24] P. Belmont, A. Aissaoui, M. Hauchecorne, N. Oudrhiri, L. Petit, J.-P. Vigneron, J.-M. Lehn, P. Lehn, *J. Gene Med.* **2002**, *4*, 517–526.
[25] X. Gao, L. Huang, *Biochem. Biophys. Res. Commun.* **1991**, *179*, 280–285.
[26] J. P. Vigneron, N. Oudrhiri, M. Fauquet, L. Vergely, J. C. Bradley, M. Basseville, P. Lehn, J. M. Lehn, *Proc. Nat. Acad. Sci. USA* **1996**, *93*, 9682–9686.
[27] S. Riebe, A. Zimmermann, J. Koch, C. Vallet, S. K. Knauer, A. Sowa, C. Wölper, J. Voskuhl, *RSC Adv.* **2020**, *10*, 19643–19647.
[28] S. Suzuki, S. Sasaki, A. S. Sairi, R. Iwai, B. Z. Tang, G. I. Konishi, *Angew. Chem. Int. Ed.* **2020**, *59*, 9856–9867.
[29] a) K. B. Steinbuch, R. I. Benhamou, L. Levin, R. Stein, M. Fridman, *ACS Infect. Dis.* **2018**, *4*, 825–836; b) K. Michael, H. Wang, Y. Tor, *Bioorg. Med. Chem.* **1999**, *7*, 1361–1371; c) I. M. Herzog, M. Feldman, A. Eldar-Boock, R. Satchi-Fainaro, M. Fridman, *MedChemComm* **2013**, *4*, 120–124.
[30] I. N. Kurniasih, H. Liang, P. C. Mohr, G. Khot, J. P. Rabe, A. Mohr, *Langmuir* **2015**, *31*, 2639–2648.

Manuscript received: October 21, 2020
Revised manuscript received: January 6, 2021
Accepted manuscript online: January 7, 2021
Version of record online: February 11, 2021